Journal of Applied Polymer Science

Thermal and mechanical properties of multiple-component aliphatic degradable polyurethanes

Rafał Poręba, Jana Kredatusová, Jiří Hodan, Magdalena Serkis, Milena Špírková
Institute of Macromolecular Chemistry AS CR, v.v.i., Heyrovského nám. 2, 162 06 Praha 6, Czech Republic
Correspondence to: M. Špírková (E-mail: spirkova@imc.cas.cz)

ABSTRACT: Macroscopic thermal and mechanical properties of complex aliphatic polycarbonate-based polyurethane (PU) films containing degradable ester units in PU backbone were studied by a combination of several experimental techniques. Differential scanning calorimetry (DSC) revealed that the synthesized oligomeric diol (DL-L) contributes (in addition to polycarbonate diol) to the formation of soft-segment domains, while the hard-segment domains are formed from 1,6-diisocyanatohexane (HDI) and butane-1,4-diol (BD). Three main phase transitions were detected by DSC and by dynamic mechanical thermal analysis. Thermogravimetric analysis (TGA) of two-component PUs showed that the PU made from DL-L and HDI is the least thermostable product, while the PU made from polycarbonate diol and HDI is the most stable one. The differences in the thermal stability of different four-component PUs are not important. Tensile properties very sensitively reflect the changes in composition and in microstructure of PU samples; the best tensile properties exhibits the degradable sample containing the equimolar ratio of hydroxyl groups of macrodiol, oligomeric diol DL-L and butane-1,4-diol. © 2015 Wiley Periodicals, Inc. J. Appl. Polym. Sci. **2015**, *132*, 41872.

KEYWORDS: differential scanning calorimetry; mechanical properties; polyurethanes; structure–property relations; thermogravimetric analysis

Received 20 August 2014; accepted 12 December 2014
DOI: 10.1002/app.41872

INTRODUCTION

The polyurethane (PU) elastomers represent very important class of PU systems. Due to excellent functional properties (tensile strength, chemical, tear and abrasion resistance, flexibility, *etc.*) they have been used for a long time in automotive industry (velocity boots) as footwear, hydraulic seals, hosed, packaging films, construction sheets, *etc.* However, PUs are promising materials also for advanced up-to-date applications, and in recent years, we witness their more and more extensive use in environment-oriented "green" technologies and in biomedical applications.[1–7] Thanks to suitable biocompatibility of PU elastomers, their controllable biodegradability and tunable elastic modulus, nowadays, they find applications as biomedical devices, temporary bones, and tissues or as degradable biomaterials.[3–7]

Three basic components are usually used for PUs preparation: "macrodiols," that is, linear oligomeric chains endcapped by hydroxyl groups (M_n mostly 1000–3000 g.mol^{-1}), low-molar-mass diols, called "chain extenders" and both aliphatic and aromatic diisocyanates.[1,2,8,9] From the chemical point of view, PUs are chemically heterogeneous multiblock copolymers. Their chains contain short blocks (segments) that differ in composition and properties. The segments containing urethane (carbamate) –NHCOO– groups, which can form strong intermolecular or intramolecular hydrogen bonds between –NH– and –CO– units, are usually called hard segments (HS) because they self-assemble in hard domains (interconnected by hydrogen bonds) which provide a sufficiently high cohesive strength of PU materials. A "pseudo" covalent structure is thus formed in bulk PU elastomers: hydrogen bonds act as fairly strong reversible crosslinks, being easily broken, and re-built by increasing or decreasing temperature. The soft rubbery segments (SS) formed mainly by macrodiol chains secure convenient material flexibility. Both types of segments are mutually incompatible and PUs form the phase-segregated structures on the nanometer scale (segregated soft- and hard-segment domains). If some other hydrogen bonds can be formed between soft and hard domain-forming segments (which depends mainly on the chemical structure of HS and SS), an additional reinforcement of PU elastomers and possible partial intermixing of different types of segments can occur. The structure and properties of PU materials are results of an intricate interplay of different thermodynamic and kinetic aspects, and therefore, a number of factors can be used to tune functional properties of PUs.

The popularity of PU elastomers actually derives from the fact that their functional properties can be easily tuned by the choice of reaction components, preparation and processing conditions. The variability of the composition of macrodiols: difference in length

and mainly in the constitution (based on polyether,[1,2,7–16] polyester,[3,5,8,9,12,15,17–19] polycarbonate,[6,16,20–29] polybutadiene[28,30,31] and their combinations[11,19,32,33]); chemical nature of diisocyanates (aromatic,[1–3,6,8,9,13,16–18,20–22,30] aliphatic[7,9,16,19,21–28,31] or cycloaliphatic[5,11,22]), and a wide choice of chain extenders (mainly short diols, as butane-1,4-diol[10,11,13,17,18,23–28,30,32]), together with the possibility to modify the preparation procedure offer an almost infinite variety in end-use (often unique) properties.

For the practical use, the usability of new materials depends on their functional properties—in this case, mainly on thermal, thermomechanical, and mechanical properties. It means that, in addition to the reproducible preparation protocol, the characterization of prepared materials and the study of their macroscopic and microscopic properties and of their structure both on large and on the nanometer scales have to be performed in great detail. The differential scanning calorimetry (DSC),[1–3,8–11,14–16,18–23,26,31,33] dynamic mechanical thermal analysis (DMTA),[1–3,8,14,17,19,21–23,25,28,31,33] thermogravimetry analysis (TGA),[1,2,8,11,14,16–20,22,26,33] and tensile characterization[1–3,8,9,12,14,15,17–19,21–23,25,31] are the most important methods of material characterization that have been widely used for studying broad diversity of macroscopic functional properties in PUE systems.

As the differences detected by above-mentioned experimental techniques on the macroscopic-scale have the origin in the behavior at the nanometer level, the analysis and interpretation of their results should be supported by methods that aim at microscopic details, such as spectroscopy (Fourier transform infrared [FTIR], NMR)[8,9,11,13,16,17,19–21,23,24,26,27,29,30,32,33,36] and microscopy (SEM, AFM, TEM) techniques.[1,8,9,14,16,18,19,21,23,24,26,27,31,33,36] Only the appropriate combination of methods of both types helps to elucidate the structure–functional property relationships in details. As concerns this paper, the discussion and interpretation of macroscopic PUE properties on large scales are based not only on pieces of information gained in this study, but also on the knowledge obtained by the multidisciplinary approach employed in our preceding study.[27]

Both DSC and DMTA provide information on structural transitions in polymer systems, such as glass transitions, melting, and crystallization processes and provide functional properties in a wide temperature range. In most cases, the temperature dependence of PUEs characteristics is complex and is influenced by many factors: PU composition, preparation procedure, curing, etc. that leads to different phase mixing/separation, morphology arrangement, ordering/crystallinity degree, *etc.*[1,2,8,9] The common thermoplastic polyurethanes containing less than 50% of HS feature three-phase transitions in the temperature range from −70 to 200°C: The transition at the lowest temperature appears mostly between −70 to −20°C and depends on the composition, length, contents of individual components, phase mixing/separation, *etc.* This transition has been generally assigned to the glass/rubber transition of soft domains.[2,11,23,25,31] The transitions between 50 to 80°C and 120 to 200°C are mostly denoted as endotherm I and II, and their assignment and unambiguous interpretation is still a question of disputes, even though both transitions have been studied deeply for several decades.[35–40] The literature is contradictory, for example, endotherm I (region 50 to 80°C) has been attributed, for example, (i) to the relaxation of chain segments in the diffused interface between soft- and hard-segment domains, (ii) to the disruption of short-range HS ordering, (iii) breaking up of the less ordered noncrystalline hard-segment domains, (iv) short-range ordering of hard-segment domains as a result of the annealing and quenching or hard-segment disordering in the boundary region between soft and hard phases.[35–40] Endotherm II (120 to 200°C) has been assigned, for example, (i) to the disruption (breakup) of long-range hard segment ordering, (ii) the disruption of various degree of short-range HS ordering, (iii) melting of microcrystalline HSD, or (iv) order-disorder transition of hard segment microdomains.[35–40]

The mechanical analysis (both static and dynamic thermal) is frequently used as a basic tool for classifying the practical utility of PC-PU elastomers and related materials. The testing of ultimate tensile properties provides simultaneously the limits of utility (strength, elongation at break, transition and decomposition temperatures, *etc.*). The DSC yields similar results as the DMTA, and it may seem that it provides redundant information. Nevertheless, DSC measurements were performed (supplemented by the thermogravimetry study) to confirm the temperature dependence of properties studied by DMTA and to gain higher confidence in data interpretation and in conclusions.

Recently, a series of new multicomponent PU elastomers containing three diols and one diisocyanate in the linear backbone was prepared. Polycarbonate-based macrodiol of M_w ca 2800 was used as the component satisfying good tensile characteristics (elongation at break, tensile strength, toughness), while the role of oligomeric diol based on *D,L*-lactide (marked as DL-L; synthesized for this purpose) was to secure regular distribution of degradable (ester) units in the PU chain. Butane-1,4-diol belongs to common chain extenders[10,11,13,17,18,23–28,30,32] and 1,6-diisocyanatohexane is more and more used diisocyanate, especially in coating and film formulations.[7,9,16,19,21–28,31] The differences in PU composition were achieved by varying molar ratio of hydroxyl groups in individual diols; the isocyanate-to-total hydroxyl ratio was kept constant and equal to 1.05. The detailed description of our multiscale approach (ranging from the segmental to micrometer levels) used for studying the complex structure, morphology, and segmental dynamic of complex PU elastomers by a combination of spectroscopy, microscopy, and scattering techniques has been published elsewhere.[27] In contrast to the previous study at the nanometer level,[27] this contribution is aimed mainly on mechanical, thermal, and thermomechanical properties of bulk multicomponent PUs (and on comparison with model two- and three-component PUs). However, the scanning electron microscopy (SEM), wide-angle X-ray diffraction (WAXD), and FTIR spectroscopy were also used in this study, because they provide direct correlation of mechanical and thermal properties with structural data and deepen the understanding of the relationship between functional properties and structural characteristics on the segmental level.

EXPERIMENTAL

Materials

The PC-based macrodiol T5652 (M_n = 2770 g mol^{-1}, kindly provided by Asahi Casei Co., Japan); 1,6-diisocyanatohexane

Table I. Codes, Composition, Hard-Segment Content and the Degree of Crystallinity of Polyurethane Elastomers

Code	Molar ratio $[OH]_{PC} : [OH]_{DL-L} : [OH]_{BD}$			HSC (wt %)	Degree of crystallinity (%)
PU-1-0-1	1	0	1	16.0	51
PU-1-1-0	1	1	0	14.6	57
PU-1-1-1	1	1	1	21.9	45
PU-1-1-2	1	1	2	28.1	43
PU-1-2-1	1	2	1	24.1	43

(HDI), butane-1,4-diol (BD), and dibutyltin dilaurate (DBTDL), all Fluka were used. "Degradable" oligomeric diol unit (DL-L, $M_n = 390$ g mol^{-1}) was prepared by ring-opening polymerization of *D,L*-lactide in solution in the presence of tin(II) 2-ethylhexanoate as catalyst and initiated by butane-1,4-diol. For further details, see Ref. 27.

Preparation Procedure. Prior to the polyaddition reaction, viscous PC and DL-L were mixed together with butane-1,4-diol, catalyst, and diisocyanate in a thoroughly dried organic solvent in order to obtain homogenous solutions. Reaction mixtures were poured into the teflon molds, and after solvent evaporation, they were put into the oven under the inert atmosphere (N_2) at 90°C for 24 h. All bulk reactions were catalyzed by DBTDL (50 ppm mol^{-1} of urethane groups) and proceeded at constant ratio of reacting groups R ($R = [NCO]/[OH]_{total} = 1.05$; $[OH]_{total} = [OH]_{PC} + [OH]_{DL-L} + [OH]_{BD}$). Different molar ratios of hydroxyl groups lead to differences in composition of individual samples, which are summarized together with sample codes in Table I, columns 1 and 2. Hard-segment content (HSC, Table I, column 3) is given in weight % of BD and HDI components with respect to the total mass of all reagents used. The final thickness of the films was 250 ± 25 μm.

Techniques of Characterization

Scanning Electron Microscopy. Surface microstructure of PU films was measured by scanning electron microscope (SEM) on the instrument Vega Plus TS 5135 (Tescan, Czech Republic). Before SEM analysis, PU films were sputtered with 4 nm Pt layer using vacuum sputter coater SCD 050 (Balzers, Czech Republic).

Differential Scanning Calorimetry. DSC analyses were carried out on a Perkin Elmer DSC 8500 calorimeter with nitrogen purge gas (20 cm^{3}min^{-1}). The instrument was calibrated for temperature and heat flow using indium as a standard. Samples of about 10 mg were encapsulated into hermetic aluminum pans. The analyses were performed in cycle heating–cooling–heating from −80°C to 200°C at 10°C min^{-1}. Two-minute isothermal plateaux were inserted before and between the ramps. The glass transition temperature is defined as a midpoint between the glassy and rubbery branches of the DSC trace and the melting temperatures as maxima of corresponding endotherm peaks. The recorded endotherm curves were evaluated as heats of melting in joules per gram.

Dynamic Mechanical Thermal Analysis. DMTA was carried out on ARES-G2 from Rheometrics Scientific (now TA instruments) using an oscillation frequency of 1 Hz, deformation ranging automatically from 0.01% (glassy state) to 3.5% (maximum deformation allowed), over a temperature range of 100 to 180°C, at a heating rate of 3°C min^{-1}. Dynamic torsion measurements were performed using rectangular samples, to which a constant tension force of 5 g was applied. The standard specimens dimensions were 25 × 6 × 0.25 mm^3. Storage modulus (G'), loss modulus (G'') and loss factor ($\tan\delta, \tan\delta = G''/G'$) were measured. In this work, the glass transition temperature (T_g) was defined as temperature of maximum value of tan δ.

Tensile Characterization. Static mechanical properties were measured on an Instron model 5800 (Instron Limited, UK) at 23°C by ISO 527 method. Dumbbell-shaped specimens (type ISO 527-2/5B; total specimen length 35 mm, length and width of the narrowed part: 12 and 2 mm, thickness 0.3 mm) and test speed 0.167 mm s^{-1} were used for the analysis. The reported values are averages obtained from at least five specimens.

Thermogravimetry. Thermogravimetric analyses (TGA) of the samples were performed on a Perkin Elmer Pyris 1 TGA. The samples were heated from room temperature to 700°C, under a nitrogen flow of 30 ml.min^{-1} at constant heating rate 10°Cmin^{-1}. Sample size in all experiments was 10–15 mg.

Wide-Angle X-ray Diffraction. Diffraction patterns were obtained using a powder diffractometer HZG/4A (Seifert GmbH, Germany) in reflection mode. The radiation Cu–Kα (wavelength $\lambda = 1.54$ Å, 40 kV, 45 mA) monochromatized with Ni foil (β filter) was used. The measurement was taken in range $2\theta = 1.4 - 40^o$ with step 0.1°, where 2θ is the scattering angle. Exposure time at each step was 10 seconds.

Fourier Transform Infrared Spectroscopy. The ATR (Attenuated Total Reflectance) FTIR spectra of the products were measured using Spectrum 100 spectrometer (Perkin Elmer) equipped with a mercury–cadmium–telluride (MCT) detector and universal ATR accessory with a diamond prism. Spectral resolution was 2 cm^{-1} with 16 scans taken for each spectrum.

RESULTS AND DISCUSSION

A series of segmented polyurethane elastomeric (PUE) films containing degradable DL-L units in the polymer backbone was successfully prepared by one-step procedure. The starting components and the building units in PUEs are given in Figure 1.

The complex character of three-component PUEs studied previously[23,25] suggested that very complex structure and properties of four-component systems can be expected. Therefore, the two-component model analogues (i.e., the products of the polyaddition reaction of 1,6-diisocyanatohexane with either polycarbonate diol, DL-L or butane-1,4-diol, marked as PU-1-0-0, PU-0-1-0, and PU-0-0-1) were also prepared, characterized, and studied. In an overwhelming majority of PU products, PC macrodiol and DL-L diol units contribute to the formation of soft domains (refer Chapter DSC) and hard domains of PUs are

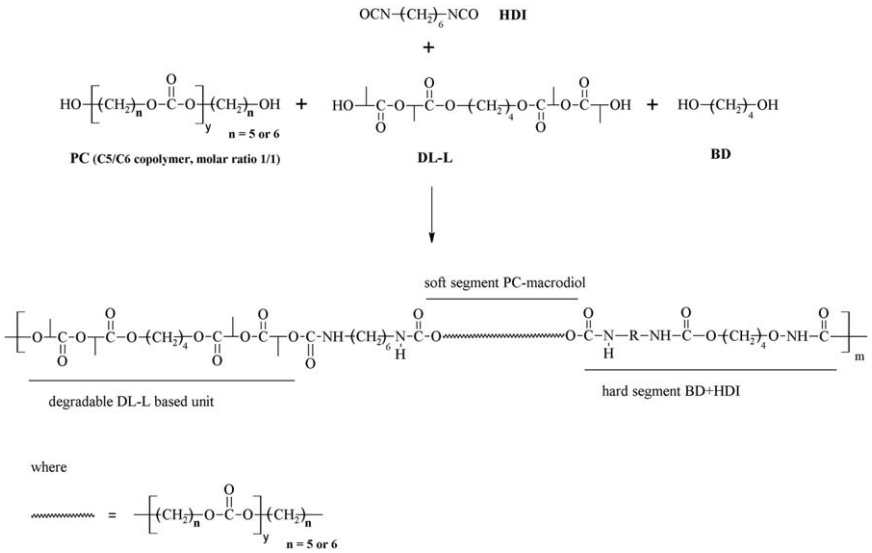

Figure 1. Starting components and basic building units in PU elastomers.

formed by the HDI-BD reaction products. However, previous detailed study of PUs on submicrometer scales (especially solid-state NMR spectroscopy) revealed that not only the structure and behavior of three- or four-component systems, but also those of two-component systems are fairly complicated.[27] This means that a currently used *a priori* sorting of building units in "pure" soft-region-building units and "pure" hard-region-building units is very approximate and generally inadequate. The present study is aimed at the confirmation of conclusions of the previous paper[27] that the behavior of a given part of PU chain depends not only on its composition, but also on the structure/interactions of/with its close surrounding. For more details, see Chapter: Solid-State NMR Characterization of PU Systems.[27] However, for simplicity, the common nomenclature based on the *a priori* classification of segments (parts of the chain formed by the addition reaction of respective units) is used in this study.

In contrast to the previous paper[27] aimed on microscopic details, this communication focuses on macroscopic functional properties, because the practical applicability of new complex PU systems is determined mainly by their macroscopic characteristics, namely by thermal, thermomechanical, and mechanical properties. Nevertheless, complementary methods (FTIR, WAXD, SEM) suitable for mapping the macroscopic characteristics onto segmental-to-micrometer level chain ordering are also used.

Scanning Electron Microscopy

The four-component PU elastomers have been developed as potential temporarily mechanically resistant, but simultaneously degradable materials for coatings and films. Their practical use requires the knowledge of the surface characteristics. As the detailed microscopy (SEM, AFM, and TEM) data of PU samples have been published elsewhere,[27] SEM characteristic and the correlation of the surface topography of films with thermal and mechanical properties are given in this communication.

SEM images of three- and four-component PU films are given in Figure 2. The differences in the overall PU topography (obtained at the magnification 500×, Figure 2 left) are not so distinct (with the exception of noticeable heterogeneous sample PU-1-1-2) unlike those obtained with magnification 5000× (Figure 2 right). At higher magnification, the surface topography is specific for each PU sample: It is evident that BD/DL-L ratio influences the surface topography of PU films. It is obvious if the following three-component samples PU-1-1-0 and PU-1-0-1, which represent the limiting compositions, are compared. While the very soft PU-1-1-0 (no BD) is self-organized in fibrillar wrinkle structures without any visible heterogeneity regions, sample PU-1-0-1 (no DL-L) is distinguished by heterogeneous surface with "scaly" formations of micrometer size regularly distributed on PU surface. The four-component PUs also mutually differ in their surface morphology: while PU-1-1-2 (the sample with the highest BD contents of all four-component PUs) is characterized by distinct scaly formations agglomerated into more-or less regular circles of μm-scale size, PU-1-1-1 and PU-1–2-1 are more homogeneous compared to PU-1-1-2 (though the circle structures of similar size and shape are outlined as well). The sample PU-1–2-1 is further characterized by visible cracks, holes, and scratches. Moreover, the self-assembly of hard-segment domains into micrometer-scale formations (spherulites) was detected inside all PU films containing BD (TEM analysis of cryo-cut and AFM analysis of freeze-fractured surfaces).[27]

Differential Scanning Calorimetry

Polycarbonate diol (PC), *D,L*-lactide-based oligomeric diol (DL-L) and three two-component model systems: PU-1-0-0 (PC product), PU-0–1-0 (DL-L product) and PU-0-0-1 (BD product) with 1,6-diisocyanatohexane were studied first by DSC. The results are given in Figure 3 and Table II.

DSC analysis of model PUs confirmed similar thermal behavior of two component PU samples based either on DL-L (PU-0–1-0) or on PC macrodiol (PU-1-0-0) but a strongly different behavior of HDI/BD system (PU-0-0-1). Since PC $T_g = -53°C$ and DL-L $T_g = -44°C$ display low glass transition temperatures,

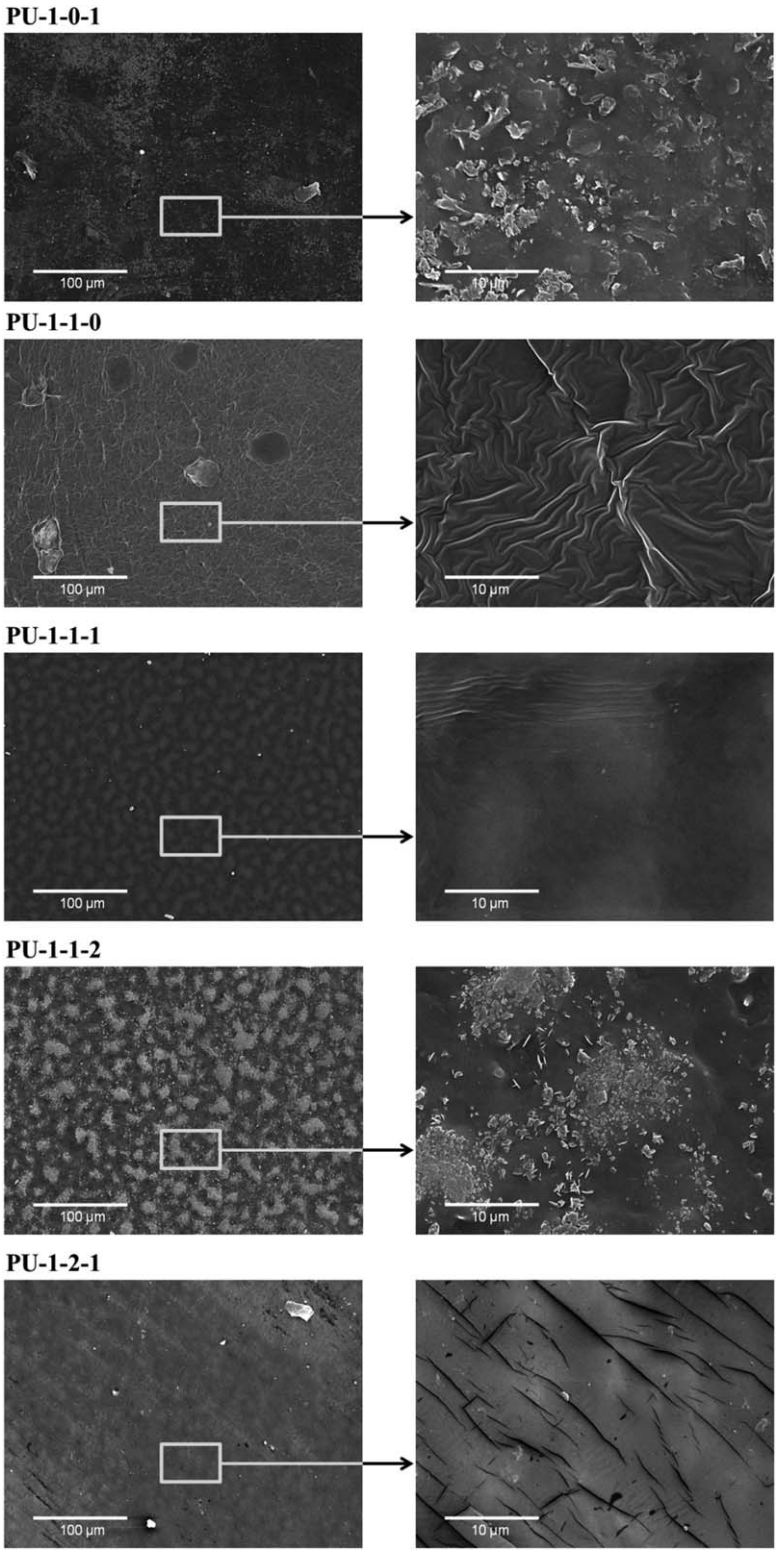

Figure 2. SEM images of surfaces of three-component (PU-1-0-1 and PU-1-0-1) and four-component (PU-1-1-1, PU-1-1-2, and PU-1–2-1) PU elastomeric films. Magnification: 500× (left) and 5000× (right). For sample code description (Table I).

the measurement suggests that both components contribute to the formation of soft domains. Moreover, the domains formed by PC or DL-L and by their products with HDI are entirely amorphous because no endotherm peaks at temperatures over 100°C were detected. On the other hand, PU-0-0-1 is a highly crystalline reaction product of BD and HDI with the melting temperature T_m= 177°C and a relaxation endotherm is detected near T_r= 60°C. The difference between the glass

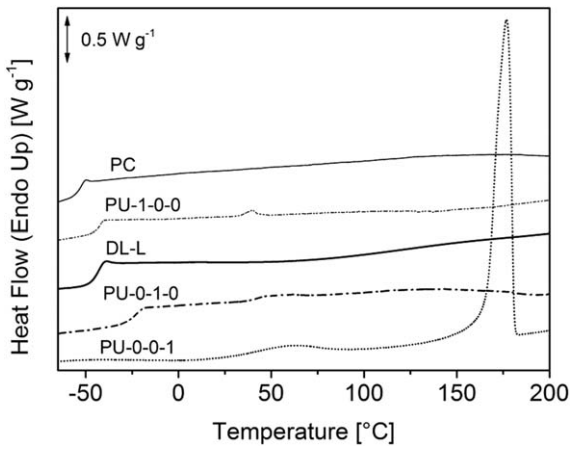

Figure 3. DSC curves of PC and DL-L diols and two-component model polyurethanes (PU-1-0-0, PU-0–1-0, and PU-0-0-1).

transition temperature of the pure soft-segment diol component and its PU product with HDI, ΔT_g, can be used for the assessment of the degree of the phase separation in the PU: the lower ΔT_g, the higher degree of the phase separation. Thereby, the sample P-1-0-0 having $T_g = -44°C$ exhibits higher degree of the phase separation $\Delta T_g = 10°C$ than P-0–1-0 one with $T_g = -26°C$ ($\Delta T_g = -18°C$). The degradable DL-L diol forms more homogenous structure than PC macrodiol if BD is missing. Since PC macrodiol has a higher M_n than DL-L diol (R ratio is constant) the number of effective interactions between urethane groups with either carbonate (PC) or ester (DL-L) groups is lower in PU-1-0-0 than in PU-0-1-0.

In the case of structurally more complex samples (marked as PU 1-X-Y (X, Y $\neq$ 0)) their T_g lie between −29 and −40°C, which indicates different degrees of the phase separation/mixing. Thermal characteristics and various transitions temperatures for selected PUs are shown in Table III (for respective DSC curves see Figure 4).

Since the composition of all samples is fairly complex (Figure. 1), the comparison of the glass transition temperatures and interpretation of their differences, ΔT_g require detailed consideration. The addition of the equimolar amount of the chain extender (PU-1-0-1) to the sample prepared without BD (i.e., PU-1-0-0) causes ΔT_g increase by 4°C. This increase correlates

Table II. Thermal Properties of Pure PC Macrodiol, DL-L Diol, and Two-Component Polyurethanes (PU-1-0-0, PU-0-1-0, PU-0-0-1)

Code	T_g (°C)	T_r (°C)	ΔH_r (J g^{-1})	T_m (°C)	ΔH_m (J g^{-1})
PC	−53	-	-	-	-
PU-1-0-0	−43	39	1	-	-
DL-L	−44	-	-	-	-
PU-0-1-0	−26	-	-	-	-
PU-0-0-1	-	60	13	177	103

T_g temperature of the glass transition, T_r second-phase transition (relaxation), ΔH_r relaxation enthalpy, T_m melting temperature of hard segments, ΔH_m melting enthalpy recorded on the first heating cycle.

Table III. Thermal Properties of Three- (PU-1-0-1, PU-1-1-0) and Four-Component Polyurethanes (PU-1-1-1, PU-1-1-2, PU-1-2-1)

Code	T_g (°C)	T_r (°C)	ΔH_r (J g^{-1})	T_m (°C)	ΔH_m (J g^{-1})
PU-1-0-1	−39	60	3	122	7
PU-1-1-0	−34	50	3	110	11
PU-1-1-1	−33	58/72	6	121	5
PU-1-1-2	−40	58	5	124	3
PU-1-2-1	−29	56/75	12	106	1

T_g temperature of the glass transition, T_r second-phase transition (relaxation), ΔH_r relaxation enthalpy, T_m melting temperature of hard segments, ΔH_m melting enthalpy recorded on the first heating cycle.

with growing number of urethane groups interacting with the carbonate groups of PC chains and immobilizing them, which results in T_g increase. The addition of BD promotes the intermixing of different units (driven hydrogen bonding). Even more remarkable ΔT_g change takes place when DL-L diol is used instead of BD in the three-component sample PU-1-1-0 ($T_g = -34°C$). However, in the case of PUs composed of two different PC and DL-L soft segments, the identification of the contributions of individual soft segments and the assignment of different interacting groups to the observed thermal effects is not possible. Anyway from the ΔT_g change in PU-1-1-0 (as compared with T_g of pure PC and DL-L), it is obvious that the phase mixing takes place in this case. DSC data show that the increasing amount of DL-L diol (in four-component PU-1-1-1 and PU-1-2-1) causes a further ΔT_g increase indicating higher tendency of DL-L chain to the overall phase mixing than of PC macrodiol. This conclusion is in accordance with DSC results of two-component PU-1-0-0 and PU-0–1-0 and SEM analysis (cf. Table II and Figure 2). On the other hand, lower T_g of PU-1-1-2 compared to the rest of four-component PUs indicates higher degree of the phase separation accompanied by noticeable heterogeneous character detected by SEM (Figure 2).

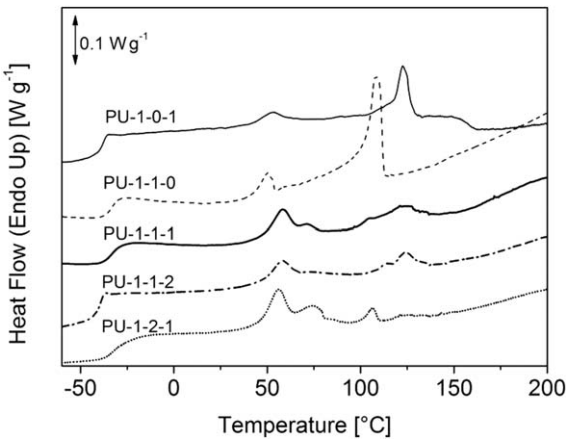

Figure 4. DSC curves of three- (PU-1-0-1, PU-1-1-0) and four-component PUs (PU-1-1-1, PU-1-1-2, PU-1–2-1). For sample code description, see Table I.

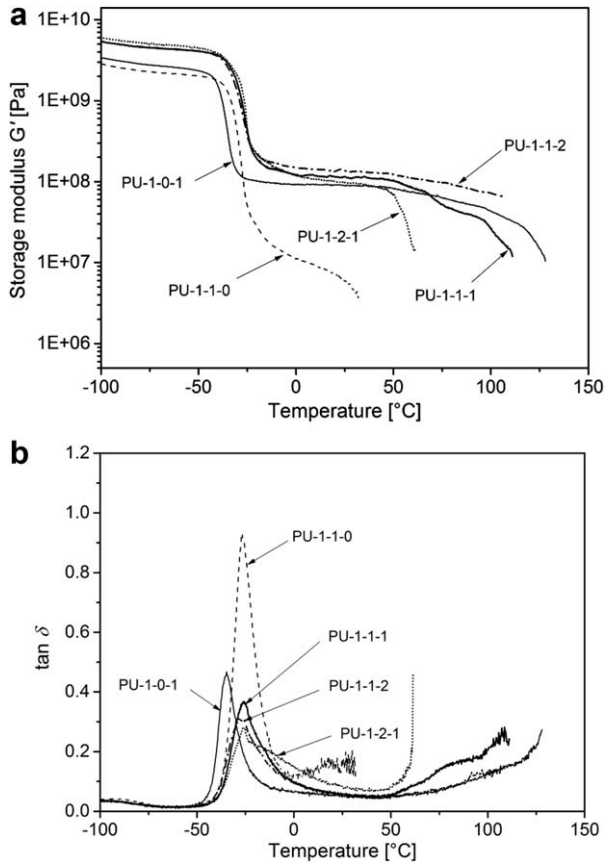

Figure 5. Temperature dependences of the storage shear modulus, G' (a) and the loss factor, tan δ, (b) of three- (PU-1-0-1, PU-1-1-0) and four-component polyurethanes (PU-1-1-1, PU-1-1-2, PU-1–2-1). For sample code description, see Table I.

A very noteworthy is the fairly surprising fact that sample PU-1-1-0 (composed merely of two different soft segments) showed the most distinct endothermic melting peak at T_m=110°C. It seems that the presence of PC macrodiol induces the crystallization/co-crystalization of low molar mass degradable DL-L diol (or vice versa). When DL-L diol was replaced with BD (PU-1-0-1), a strong endothermic crystalline peak was slightly shifted toward higher temperature T_m=122°C. This endotherm has been ascribed to the melting of hard segment domains formed from HDI/BD units. In the case of PU samples composed of DL-L and BD (PU-1-1-1 or PU-1–2-1), both peaks (T_m=110 and 122°C) are present in the form of more complex, multiple endotherms, while in PU-1–2-1, containing the excess of D,L-L, the magnitude (i.e., the heat effect) of the higher temperature endotherm (T_m=122°C) decreased considerably.

Additional endothermic peaks are visible in the region between 50–75°C (Figure 4). Three-component sample PU-1-0-1 is characterized by relatively low relaxation enthalpy (ΔH_r=3Jg^{-1}) with the maximum at 60°C (Table III). If BD is replaced by DL-L diol in three-component PU-1-1-0, the relaxation endotherm occurs at a lower temperature (by ca. 10°C), but ΔH_r value remains the same (cf. lines 1 and 2 in Table III). On the other hand, two distinguishable endotherms are found in four-component samples as a result of combination of both components, DL-L and BD. Since the particular values of relaxation enthalpies ΔH_r increase with decreasing melting enthalpies ΔH_m (Table III, 4th and 6th columns), the endotherms can be ascribed to the relaxation processes of amorphous phases of the polyurethane matrix. Lower degrees of crystallinity detected by WAXD for the four-component systems compared to three-component counterparts can be regarded to as supporting information for this reasoning (see Chapter WAXD and Table I, 4th column).

Dynamic Mechanical Thermal Analysis

The mechanical properties of PU samples under dynamic conditions were studied by DMTA. The temperature dependences of the storage shear modulus G' and loss factor tan δ are shown in Figure 5. From the temperature dependence of the loss factor tan δ, it follows that the first local segmental motions of chains (β transition) occur at ca. −80°C in all cases. The next observed transition is the glass transition detected at the peak maximum of the loss factor tan δ, that is, at the glass transition temperature T_g which depends on particular sample composition. The lowest T_g of about −35°C was found for the sample based merely on PC macrodiol and BD (PU-1-0-1). The replacement of BD by DL-L in PU-1-1-0 results in T_g shift to higher temperature, −26°C, indicating a stronger interaction of DL-L with PC chains than that of BD with PC in the sample PU-1-0-1 (ΔT_g between these two samples is 9°C). Thereby, it can be concluded that PU-1-1-0 is more homogenous material than PU-1-0-1 one, which is in accordance with SEM and DSC results. Since DL-L products do not contain both groups necessary for the formation of H-bonds, there segments interact predominantly only via dipole–dipole interactions. The number of strong H-bonds originating from urethane linkages is thus negligible and the sample PU-1-1-0 is characterized by very low values of storage modulus G'. Moreover, the lack of strong physical cross-links causes that PU-1-1-0 starts to melt at around 30°C. It is noteworthy that despite the loss of its elastomeric properties, the sample still keeps an important fraction of nanocrystalline domains in the viscous state. These domains

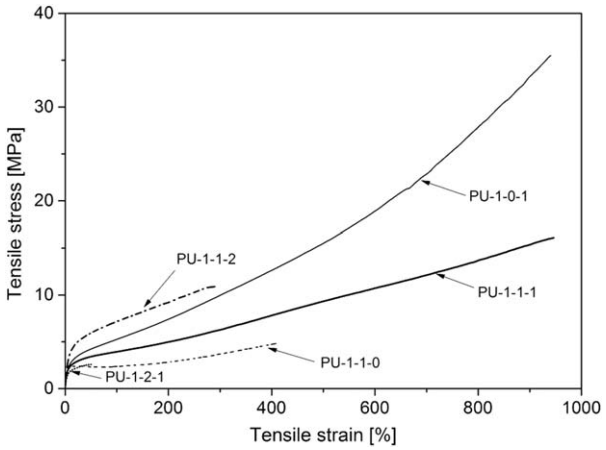

Figure 6. Stress–strain dependences of three- (PU-1-0-1, PU-1-1-0) and four-component polyurethanes (PU-1-1-1, PU-1-1-2, PU-1–2-1). For sample code description, see Table I.

Table IV. Selected Tensile Properties and h_{rel} of Three- (PU-1-0-1, PU-1-1-0) and Four-Component Polyurethanes (PU-1-1-1, PU-1-1-2, PU-1–2-1)

	Tensile strength (MPa)	Elongation at break [%]	Young's modulus (MPa)	M100 [MPa]	M300 (MPa)	Toughness (mJ mm^{-3})	$h_{rel}^* = h_1/h_2$
PU-1-0-1	34.0 ± 6.1	965 ± 30	56.7 ± 3.5	5.2 ± 0.1	9.6 ± 0.5	156.2 ± 19	1.69
PU-1-1-0	4.6 ± 0.3	398 ± 27	62.8 ± 1.3	2.5 ± 0.02	3.8 ± 0.03	12.8 ± 1.1	5.52
PU-1-1-1	16.5 ± 1.0	964 ± 46	55.3 ± 2.9	3.9 ± 0.04	6.3 ± 0.1	91.2 ± 6.3	1.82
PU-1-1-2	9.4 ± 1.8	289 ± 43	83.0 ± 3.5	7.1 ± 0.1	-	23.1 ± 5.0	1.08
PU-1-2-1	1.8 ± 0.3	67 ± 3	44.0 ± 0.6	---	-	1.7 ± 0.1	2.29

h_{rel}^* is explained and discussed in Chapter FTIR.

melt completely at quite high temperature of 110°C (cf. Table I, Figure 4 and Figure 9).

The broadest rubbery region with the highest melting temperature (covering ~150°C) was found for the sample PU-1-0-1 prepared from PC and BD. The addition of the equimolar amount of DL-L (PU-1-1-1) to this sample results in a slight increase in storage modulus and T_g; however, the melting temperature slightly decreases, and hence, the rubbery plateau is also reduced.

If more BD is added (PU-1-1-2), almost no change either in T_g or T_m occurs in comparison with PU-1-1-1. Only the storage modulus G' slightly increases. However, a twofold amount of DL-L (relative to BD) in the sample PU-1–2-1 causes the melting at around 60°C and the glass transition at −25°C, which results in the narrowest rubbery region of the four-component PUs. The data suggest that in PU-1–2-1 the dipole–dipole interactions between DL-L segments and PC macrodiol chains play very important role and their effect probably exceeds the contribution of H-bonds arising from the hard segment domains composed of BD and HDI.

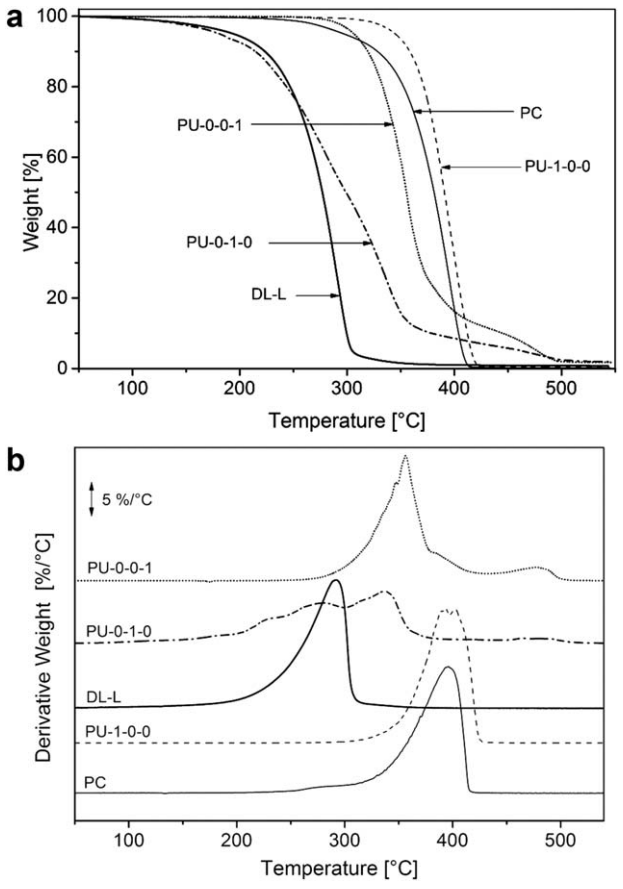

Figure 7. TG (a) and DTG decomposition curves (b) of starting PC and DL-L diols and model two-component polyurethanes (PU-1-0-0, PU-0–1-0, and PU-0-0-1).

Tensile Properties

Tensile properties depend substantially on the composition PU samples (Figure 6 and Table IV). Sample PU-1-1-1 exhibits the strain at break and tensile strength ca. twice lower than PU-1-0-1, the sample without any DL-L. This fact can be explained by the lower content of carbonate carbonyl groups in PU-1-1-1 that are important for the formation of hydrogen bonds (in addition to urethane hydrogen bonds) which play a role of temporary cross-linking junctions. Very interesting product is the soft sample PU-1-1-0 containing no butane-1,4-diol. This PU has relatively high Young modulus, but it is very soft. Unlike others PUs, PU-1-1-0 contents the yield point at ca. 10% of elongation. (The yield point is typical feature for the fibrillar materials. SEM analysis of sample PU-1-1-0 confirmed self-organized fibrillar structures on the surface; Figure 2).

PU prepared in the presence of BD (PU-1-0-1) shows the highest value of tensile strength at around 34 MPa and an extraordinary high strain at break of ca 965%. The replacement of BD by degradable DL-L linkage (sample PU-1-1-0) results in a significant decrease in both values of the ultimate strength and strain at break. This suggests that DL-L based segments linked with 1,6-diisocyanatohexane are incapable to form domain structures acting as cross-linking sites. This can be a result of the steric hindrance that prevents the formation of strong H-bonds between urethane groups.

However, the dipole–dipole interactions are predominating forces controlling the microstructure of PU-1-0-1. The reduction of tensile strength of PU-1-1-1 (containing equal molar concentrations of all hydroxyl groups) as compared to PU-1-0-1 can be explained by the same arguments. However, the introduction of DL-L reduces the number of BD molecules participating in hard-segment formation, and thus, tensile strength is diminished. Further increase in BD concentration, as in the sample PU-1-1-2 leads to the considerable decrease in all tensile characteristics (except the Young modulus). The excess of BD

increases the hard segment content (and increases the number of urethane H-bonds), but simultaneously, it causes that the samples are tougher and more brittle. Similar influence of HS content on mechanical properties was observed in our previous studies.[23,25] The excess of DL-L (i.e., in sample PU-1-2-1), the tensile strength falls to the lowest value of ~1.8 MPa and strain at break is around 70%. Low values of macroscopic characteristics are related to distinct cracks and scratches detectable on the surface detected by SEM (Figure 2). Toughness of PU-1-2-1 is thus nearly hundred-times lower compared to PU-1-0-1. From the practical point of view, degradable PU sample containing the equimolar ratio of hydroxyl groups of all diols (PU-1-1-1) is the best candidate of four-component PUs, due to sufficient tensile properties.*

The correlations of tensile properties with FTIR results will be further discussed in the Chapter FTIR.

Thermogravimetry

The thermal stability of PC and DL-L, two-component model PUs and complex PU samples were studied by TGA. The weight loss and the derivative of the weight loss of the pure DL-L, PC, and their two-component products with HDI are given in Figure 7 as functions of temperature. As shown in Figure 7, the least thermally stable component is the degradable DL-L diol. The product of the reaction with HDI (PU-0-1-0) exhibits a slightly extended, although relatively complex, decomposition pattern with the maximum decomposition rate at around 345°C. The reason for increased stability is the presence of more stable HDI linkages assisting in heat energy dissipation and hence improving material stability. PC macrodiol is the most stable component (maximum decomposition rate at around 395°C) and the reaction product with HDI remains nearly unchanged. The pure hard segment (i.e., BD/HDI product, PU-0-0-1) shows the maximum decomposition rate at 360°C and lies somewhere between DL-L diol and and PC macrodiol.

The decomposition patterns (and their derivatives) of three- and four-component PUs are shown in Figure 8, while T_{max1}, T_{max2}, $T_{5\%}$ and $T_{10\%}$, and Δm values for the PU samples are given in Table V.

The most thermally stable ($T_{5\%}$=314°C) is the sample PU-1-0-1 based merely on PC macrodiol, HDI and BD (Table V). All PU samples containing DL-L are distinguished by lower thermal stability compared to PU-1-0-1, due to low thermal stability of pure DL-L (Figure 7). The lowest $T_{5\%}$ was detected for DL-L rich sample PU-1-2-1 and further for PU-1-1-0 (257°C and 266°C, respectively), both products starting with the decomposition process just above 200°C. The same situation concerns remaining PU samples containing degradable DL-L units. However, if lower amount of DL-L is present, a slight improvement of thermal stability is observed (samples PU-1-1-1 and PU-1-1-2). Nearly, identical trend is observed when temperatures at which 10 wt % loss of the total mass are compared. On the other hand, the temperatures at which the maximum loss of

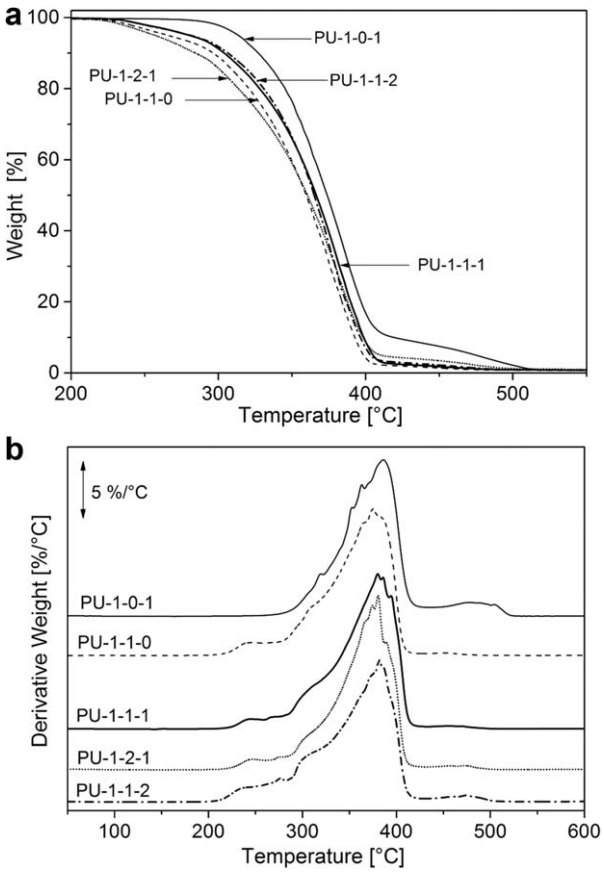

Figure 8. TG (a) and DTG decomposition curves (b) of three- (PU-1-0-1, PU-1-1-0) and four-component polyurethanes (PU-1-1-1, PU-1–2-1, and PU-1-1-2). For sample code description, see Table I.

weight is observed ($T_{max\ 1}$ and $T_{max\ 2}$) are fairly similar. Thus, it seems that the presence of PC macrodiol (regardless of its amount) imparts better thermal stability to all degradable PUs. Similar thermal stability of all samples containing DL-L can be caused by the fact that all mass loss changes start at temperatures above 200°C. At high temperatures, all samples are in the form of viscous liquids, because all crystalline domains already melted and other ordered formations have been already destroyed (cf. Chapters DSC and DMTA). As the weight percentages of individual components are relatively similar in all PU samples, the differences in thermal stabilities are low.

Functional properties of PU elastomers depend on a number of factors, such as chemical nature of starting components (macrodiol, diisocyanate, chain extender), the contents and length of the soft and hard segments, the strength of hydrogen bonds and dipole–dipole interactions, the degree of the phase separation/mixing, the mobility and orientation (packing) of building units within the hard segments, overall reaction conditions during PU preparation, temperature profile, *etc.* and it is dangerous to formulate the general conditions in a broad context. Nevertheless, the performed study established that thermal stability of PUs containing degradable oligomeric diol (DL-L) is lower than that of the PU elastomers and PU nanocomposites studied previously,[23,25,31] This fact is caused by the relatively low thermal

*Current long-time tests of degradability of PU-1-1-1 confirmed DL-L efficiency in the degradation process.

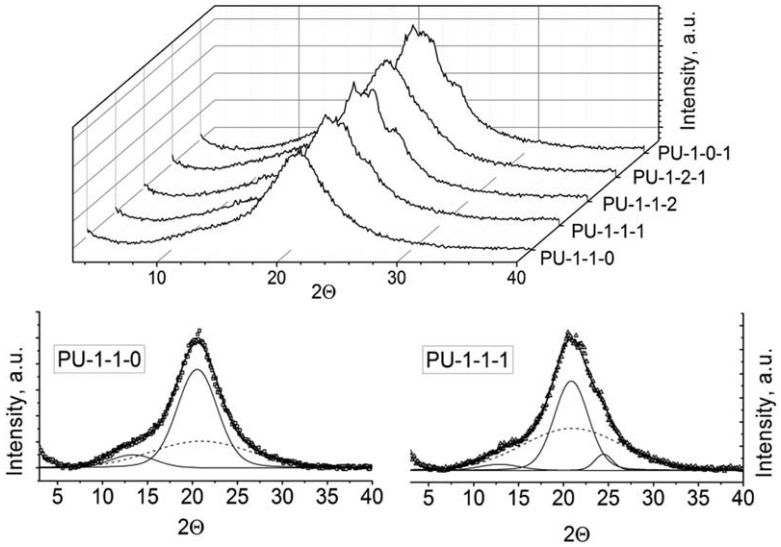

Figure 9. WAXD profiles of three- (PU-1-0-1, PU-1-1-0) and four-component polyurethanes (PU-1-1-1, PU-1-1-2, PU-1-2-1; top). Examples of evaluation of the amorphous and crystalline portion (bold line—fitting curve; thin line—crystalline peak; dashed line—amorphous halo) for three-component PU-1-0-1 (bottom left) and four-component PU-1-1-1 (bottom right). For sample code description, see Table I. (The size of all crystals in PU samples is mostly (ca 90%) about 2 nm and in the minority (ca 10%) about 4 nm).

stability of DL-L. Compared to PU and PU nanocomposites,[23,25,31] mechanical properties are also deteriorated, due to the decrease in quantity (or intensity) of H-bonds and dipole–dipole interactions in PUs containing DL-L. Anyway, the functional properties of four-component sample PU-1-1-1 are suitable for the intended use (as temporary degradable films).

Wide-Angle X-ray Diffraction

WAXD experiments have been performed as a complementary method to DSC analysis. WAXD profiles of PU samples are shown in Figure 9. All PU samples tested exhibit very high degree of the crystallinity, between 43 and 57%, see Table I, 4th column. As the three- or four-component PU samples contain at most 30% of the hard segments, it is obvious that the *a priori* soft segments (i.e., PC or DL-L units) have to contribute to the overall degree of crystallinity. This assumption is in accordance with the solid-state NMR spectroscopy results (Chapter: Solid-State NMR Characterization of PU Systems in Ref 27). It is worth-emphasizing that the highest degree of crystallinity was found for the sample PU-1-1-0, that is, the sample without any BD and without any long-range ordering, which is in accordance with DSC experiments (cf. Figure 4 and Table III). The three-component PUs have a higher degree of crystallinity than the four-component PUs (Table I, 4th column). This can be explained by more regular arrangement of segments constituting the PU chain which can lead to higher degrees of the arrangement of parts of chains in crystalline nanodomains in the case of simpler three-component PU samples as compared with more complex and more chemically and structurally heterogeneous four-component samples.

Table V. The Thermal Stability of Three- (PU-1-0-1, PU-1-1-0) and Four-Component Polyurethanes (PU-1-1-1, PU-1-1-2, PU-1-2-1)

Code	T_{max1} (°C)	Δm_1 (wt %)	T_{max2} (°C)	Δm_2 (wt %)	$T_{5\%}$ (°C)	$T_{10\%}$ (°C)
PU-1-0-1	387	91	489	8	314	327
PU-1-1-0	378	98	455	1	266	296
PU-1-1-1	386	98	460	1	281	304
PU-1-1-2	380	97	466	2	281	307
PU-1-2-1	381	96	470	3	257	285

T_{max}—the temperature at the DTG curve maximum; $T_{5\%,\ 10\%}$—the temperature at which the lost of 5%, respectively, 10%, of the total sample mass occurred. Δm—the weight loss.

Fourier Transform Infrared Spectroscopy

FTIR was used mainly for studying the conversion of isocyanate groups, chemical structure of PUs and hydrogen bond formation.[27] In this contribution, FTIR was also employed to correlate different tensile properties with PU structure. As the tensile characteristics are strongly influenced by the number and strength of hydrogen bonds between amino- and carbonyl groups present in the complex PUs, the attention was paid to the spectral region of carbonyl stretching vibrations from 1600 to 1800 cm^{-1}, highlighted in Figure 10a.

All PU samples are composed of soft segments (arising either from PC-macrodiol or oligomeric DL-L) and hard segments (HDI+BD reaction products). In the previous contribution,[27] the assignment of the peak position of free carbonyl of the soft segment (1739 cm^{-1}) and of carbonyl of urethane in the hard segment (1684 cm^{-1}) was presented. In this contribution, the ratios of intensities of peak at 1739 cm^{-1} (h_1) and at 1684 cm^{-1} (h_2; for the definition, see Figure 10b), are correlated with ultimate values of the stress and elongation of all three- and four-component PUs with a special emphasis on DL-L and BD molar ratio in PU formulations.

If tensile strength and elongation at break are correlated with the fraction of hydrogen bonds (i.e., if h_{rel} are plotted versus σ_b

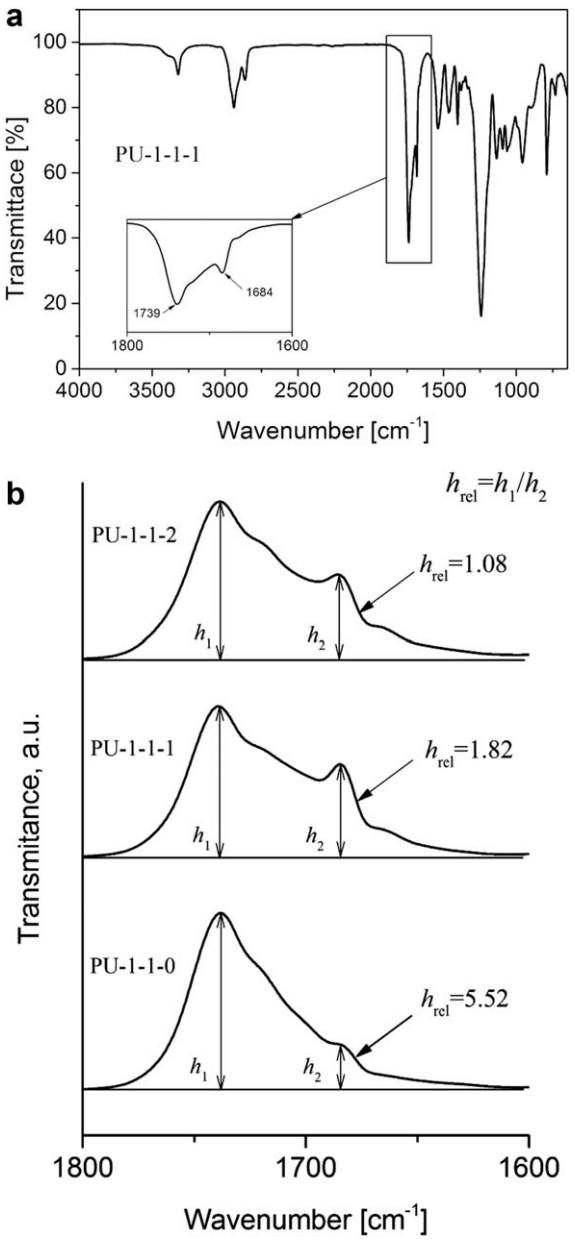

Figure 10. FTIR spectra of PU-1-1-1 with highlighted carbonyl stretching region (a), carbonyl stretching vibrations of PU samples with different BD concentrations, from the top to the bottom: PU-1-1-0, PU 1-1-1, PU1-1-2 (b). The contribution of the soft- and hard-segment intensities is indicated by ratio $h_{rel}=h_1/h_2$.

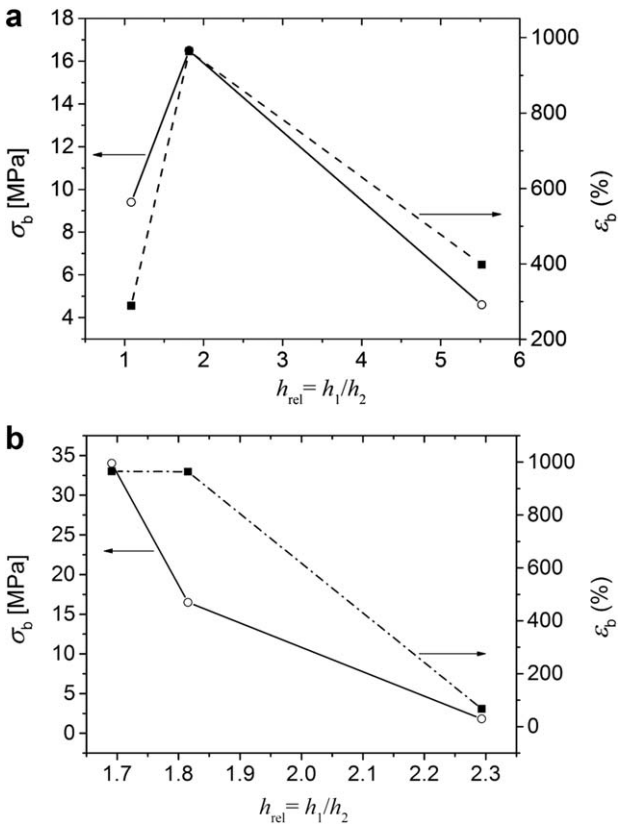

Figure 11. The dependences of tensile strength (σ_b; full lines) and elongation at break (ε_b; broken lines) on h_{rel} for PU samples with different BD molar ratio: PU-1-1-0, PU-1-1-1, and PU1-1-2 (a) and different molar DL-L ratio: PU-1-0-1, PU-1-1-1, and PU-1–2-1 (b). For sample code description, see Table I. (For further details, see also Figure 10b and Table IV, 8th column).

and ε_b for different BD (Figure 11a) and different DL-L molar ratio (Figure 11b), it is evident that the values of ultimate tensile properties strongly depend on h_{rel}. Tensile properties reach the maximum values if the optimum fraction of hydrogen bonds is achieved, that is, for h_{rel} close to 1.8.

CONCLUSIONS

Thermal and mechanical properties of complex polyurethane elastomers containing two components contributing to soft segments formation and two components contributing to the hard segments formation have been studied by a number of experimental techniques. The complexity of the thermal and mechanical behavior is a result of complex self-assembling processes leading to the segregation and arrangement of chemically different parts of PU chains in soft and hard domains. The use of short oligomeric *D,L*-lactide-based diol (containing on average four ester groups in each molecule) enabled the incorporation of units prone to the degradation process in the PU backbone. The addition of DL-L was accompanied by the decrease in the thermal stability and the degree of phase separation (to some extend) and by substantial deterioration of tensile properties (in most cases), which is undesirable, because tensile properties limit the applicability the PU elastomers.

The study indicates that FTIR spectroscopy can be used as a useful tool for tuning the tensile characteristics: Careful comparison of results of different experimental techniques shows that suitable end-use properties require an optimum fraction of hydrogen bonds. Because the carbonyl stretching vibrations of soft-segment and hard-segment components provide information on hydrogen bonds, they appear to be a good gauge for tailoring the ultimate tensile properties of polyurethanes with the equimolar ratio of hydroxyl groups from macrodiol, oligomeric diol, and butane-1,4-diol with respect to $[NCO]/[OH]_{total}$ ratio. The study shows that PUs with the equimolar content of diols are particularly suitable for potential practical use, because they exhibit optimum combination of all macroscopic characteristics as detected by DSC, TGA, and DMTA and tensile

properties. PUs containing higher contents of degradable DL-L oligomer (double in four-component PU or in three-component PU without any butane-1,4-diol) melt and form viscous fluid at low temperatures (30 to 60°C, depending on composition). However, it was found that these PUs surprisingly contain fairly high fractions of nanocrystalline structures in the viscous state at elevated temperatures. These nanocrystallites melt at fairly high temperatures (over 100°C), as detected by DSC in three-component PU sample without any butane-1,4-diol. Oligomeric DL-L diol was identified as the most prone component to the thermal degradation process and polycarbonate macrodiol as the least prone component to degradation. The decomposition of PU starts at about 250°C, depending on the composition. Detailed FTIR, WAXD, and SEM experiments confirmed that the source of the diversity of macroscopic mechanical and thermal properties of complex PU systems unwinds from differences between microstructures formed already at the segmental, nanometer and micrometer levels.

ACKNOWLEDGMENTS

The authors thank the financial support of the Grant Agency of the Czech Republic (Czech Science Foundation, project no. 13-06700S). The experimental work of L. Machová (DL-L synthesis), I. Vlasáková (DMTA), and Dr. A. Zhigunov (WAXD) is acknowledged as well.

REFERENCES

1. Buist, J. M. Developments in Polyurethane-1; Applied Science Publishers Ltd.; London, **1978**.
2. Hepburn, C. Polyurethane Elastomers, 2nd ed.; Elsevier Science Publisher Ltd.; England, **1992**.
3. Dempsey, D. K.; Robinson, J. L.; Iyer, A. V.; Parakka, J. P.; Bezwada, R. S.; Cosgriff-Hernandez, E. M. *J. Biomater. Sci. Polym. Ed.* **2014**, *25*, 535.
4. Mercado-Pagan, A. E.; Kang, Y. Q.; Ker, D. F. E.; Park, S.; Yao, J.; Bishop, J.; Yang, Y. P. *Europ. Polym. J.* **2013**, *49*, 3337.
5. Moravek, S. J.; Hassan, M. K.; Drake, D. J.; Cooper, T. R.; Wiggins, J. S.; Mauritz, K. A.; Storey, R. F. *J. Appl. Polym. Sci.* **2010**, *115*, 1873.
6. Xu, Y. S.; Wu, X. Y.; Xie, X. Y.; Zhong, Y. P.; Guidon, R.; Zhang, Z.; Fu, Q. *Polymer* **2013**, *54*, 5363.
7. Baudis, S.; Ligon, S. C.; Seidler, K.; Weigel, G.; Grasl, C.; Bergmeister, H.; Schima, H.; Liska, R. *J. Polym. Sci. Part A: Polym. Chem.* **2012**, *50*, 1272.
8. Petrović, Z. S.; Ferguson, J. *Prog. Polym. Sci* **1991**, *16*, 695.
9. Prisacariu, C. Polyurethane Elastomers. From Morphology to Mechanical Aspects; Springer Wien: New York, **2011**.
10. Vilas, J. L.; Laza, J. M.; Rodriguez, C.; Rodriguez, M.; Leon, L. M. *Polym. Eng. Sci.* **2013**, *53*, 744.
11. Cakić, S. M.; Ristić, I. S.; Krakovský, I.; Stojiljković, D. T.; Bělský, P.; Kollová, L. *Mater. Chem. Phys.* **2014**, *144*, 31.
12. Ma, R. Y.; Yi, Y. H. *Mater. Eng Technol. Book Series Adv. Mater. Res.* **2014**, *849*, 261.
13. Nachman, M.; Kwiatkowski, K. *Wear* **2013**, *306*,113.
14. Choi, M. C.; Jung, J. Y.; Yeom, H. S.; Chang, Y. W. *Polym. Eng. Sci.* **2013**, *53*, 982.
15. Chang, C. H.; Tsao, C. T.; Chang, K. Y.; Chen, S. H.; Han, J. L; Hsieh, K. H. *Bio-Med. Mater. Eng.* **2012**, *22*, 373.
16. Rogulska, M.; Kultys, A.; Olszewska, E. *J. Therm. Anal. Calorim.* **2013**, *114*, 903.
17. Li, C. B.; Che, R. S.; Xiang, J.; Lei, J. X.; Zhou, C. L. *J. Appl. Polym. Sci.* **2014**, 131.
18. Anandhan, S.; Lee, H. S. *J. Elastom. Plast.* **2014**, *46*, 217.
19. Zeng, C.; Zhang, N. W.; Ren, J. *J. Appl. Polym. Sci.* **2012**, *125*, 2564.
20. Cipriani, E.; Zanetti, M.; Brunella, V.; Costa, L.; Bracco, P. *Polym. Degrad. Stabil.* **2012**, *97*, 1794.
21. Fernandez-d'Arlas, B.; Corcuera, M.; Runt, J.; Eceiza, A. *Polym. Int.* **2014**, *63*, 1278.
22. Panwiriyarat, W.; Tanrattanakul, V.; Pilard, J. F.; Pasetto, P.; Khaokong, C. *J. Appl. Polym. Sci.* **2013**, *130*, 453.
23. Špírková, M.; Pavličević, J.; Strachota, A.; Poręba, R.; Bera, O.; Kapráková, L.; Baldrian, J.; Šlouf, M.; Lazić, N.; Budinski-Simendić, J. *Europ. Polym. J.* **2011**, *47*, 959.
24. Špírková, M.; Poręba, R.; Pavličević, J.; Kobera, L.; Baldrian, J.; Pekárek, M. *J. Appl. Polym. Sci.* **2012**, *126*, 1016.
25. Poręba, R.; Špírková, M.; Brožová, L.; Lazić, N.; Pavličević, J.; Strachota, A. *J. Appl. Polym. Sci.* **2013**, *127*, 329.
26. Poręba, R.; Špírková, M.; Pavličević, J.; Budinski-Simendić, J.; Szeczenyi, K. M.; Hollo, B. *Compos. B* **2014**, *58*, 496.
27. Špírková, M; Machová, L.; Kobera, L.; Brus, J.; Poręba, R.; Serkis, M.; Zhigunov, A. *J. Appl. Polym. Sci.* **2015**, *132*, 41590.
28. Kuta, A.; Hrdlička, Z.; Strachota, A.; Špírková, M. *Mater. Manuf. Process.* **2009**, *24*, 1214.
29. Eceiza, A.; Martin, M. D.; De la Caba, K.; Kortaberria, G.; Gabilondo, N.; Corcuera, M. A.; Mondgragon, I. *Polym. Eng. Sci.* **2008**, *48*, 297.
30. Fazal-ur-Rehman,; Bhatti, I. A.; Zuber, M.; Bhatti, H. N.; Asgher, M. *Asian J. Chem.* **2011**, *23*, 880.
31. Špírková, M.; Duszová, A.; Poręba,; R.; Kredatusová, J.; Bureš, R.; Fáberová, M.; Šlouf, M. *Compos. B* **2014**; *67*, 434.
32. Li, G. Y.; Li, D. D.; Niu, Y. Q.; He, T.; Chen, K. C.; Xu, K. T. *J. Biomed. Mater. Res. A* **2014**, *102*, 685.
33. D'Arlas, B. E.; Rueda, L.; De la Caba, K.; Mondragon, I.; Eceiza, A. *Polym Eng. Sci.* **2008**, *48*, 519.
34. Mi, H. Y.; Li, Z.; Turng, L. S.; Sun, Y. G.; Gong, S. Q. *Mater. Design.* **2014**, *56*, 398.
35. Seymour, R. W; Cooper, S. L. *Macromolecules* **1973**, *6*, 48.
36. Kultys, A.; Rogulska, M.; Pikus, S.; Skrzypiec, K. *Eur. Polym. J.* **2009**, *45*, 2629.
37. Hesketh, T. R; Van Bogart, J. W. C.; Cooper, S. L. *Polym. Eng. Sci.* **1980**, *20*, 190.
38. Jin, J.; Song, M.; Yao, K. J. *Thermochim. Acta* **2006**, *447*, 202.
39. Finnigan, B.; Mattin, D.; Halley, P.; Truss, R.; Campbell, K. *Polymer* **2004**, *45*, 2249.
40. Koberstein, J. T.; Russell, T. P. *Macromolecules* **1986**, *19*, 714.